Articles

Importance of Factor VIIa Gla-Domain Residue Arg-36 for Recognition of the Macromolecular Substrate Factor X Gla-Domain†

Wolfram Ruf,‡ Justin Shobe,‡ S. Mohan Rao,§ Craig D. Dickinson,‡,|| Arthur Olson,§ and Thomas S. Edgington*,‡

Departments of Immunology and Vascular Biology and Department of Molecular Biology, The Scripps Research Institute, La Jolla, California 92037

Received September 18, 1998; Revised Manuscript Received November 16, 1998

ABSTRACT: Macromolecular substrate docking with coagulation enzyme−cofactor complexes involves multiple contacts distant from the enzyme's catalytic cleft. Here we characterize the binding of the Gla-domain of macromolecular substrate coagulation factor X to the complex of tissue factor (TF) and VIIa. Site-directed mutagenesis of charged residue side chains in the VIIa Gla-domain identified Arg-36 as being important for macromolecular substrate docking. Ala substitution for Arg-36 resulted in an increased K_M and a decreased rate of X activation. X with a truncated Gla-domain was activated by mutant and wild-type VIIa at indistinguishable rates, demonstrating that Arg-36 interactions require a properly folded Gla-domain of the macromolecular substrate. VIIa Arg-36 was also required for effective docking of the X Gla-domain in the absence of phospholipid, demonstrating that the Gla-domain of VIIa participates in protein−protein interactions with X. In the absence of TF, the mutant VIIa had essentially normal function, indicating that the cofactor positions VIIa's Gla-domain for optimal macromolecular substrate docking. Computational docking suggests multiple charge complementary contacts of the X Gla-domain with TF·VIIa. A prominent interaction is made by the functionally important X residue Gla-14 with the center of the extended docking site created by residues in the carboxyl module of TF and the contiguous VIIa Gla-domain. These data demonstrate the functional importance of interactions of the Gla-domains of enzyme and substrate, and begin to elucidate the molecular details of the ternary TF·VIIa·X complex.

Proteases of the coagulation system are dependent on protein cofactors that enhance proteolytic function and direct macromolecular substrate specificity (*1*). The cofactors not only influence the catalytic cleft of the bound proteases but also support the proper docking of macromolecular substrate for optimal scissile bond presentation to the enzyme. Indeed, recent studies indicate that macromolecular substrate docking, i.e., the binding of substrate with multiple sites in the enzyme and/or cofactor, is independent of, and even precedes, scissile bond docking and cleavage (*2*). The cofactor−enzyme complex of tissue factor (TF)[1] with coagulation factor VIIa (VIIa) initiates the coagulation pathways, ensures normal hemostasis, and is involved in the pathogenesis of a variety of pathological processes, including septic shock, thrombotic vascular disease, and cancer metastasis (*3*). The availability of extensive mutagenesis data (*4*, *5*) and the structure of the TF·VIIa complex (*6*) makes this enzyme−cofactor complex well suited for detailed analysis of the precise mode of macromolecular substrate docking.

VIIa has an unusually low amidolytic activity that is enhanced upon formation of the TF·VIIa complex. TF likely supports a labile zymogen to enzyme transition of the VIIa protease domain, thus enabling full catalytic function of the enzyme when it is bound to cofactor (*5*, *7*). The enhancement of amidolytic activity of VIIa in the presence of TF, however, does not fully account for the accelerated rate of macromolecular substrate factor X (X) activation. The more efficient cleavage of X is rather a consequence of facilitated docking with TF·VIIa, ultimately accelerating scissile bond cleavage and product formation. Several structural domains are inferred to be involved in the macromolecular substrate docking, although the precise details are poorly defined in the absence of crystallographic data for the ternary TF·VIIa·X complex.

The Gla-domain of X has been implicated in the interaction with TF·VIIa, on the basis of the following evidence. First, hereditary X mutants with a Gla-7 → Gly (*8*) or Gla-14 →

† This work was supported by NIH Grant PO1-HL16411 and performed during the tenure of an Established Investigator Award of the American Heart Association (to W.R.).

* Corresponding author: Departments of Immunology and Vascular Biology, IMM-17, 10550 N. Torrey Pines Rd., La Jolla, CA 92037. Telephone: (619) 784-8225. Fax: (619) 784-8480. E-mail: tse@scripps.edu.

‡ Departments of Immunology and Vascular Biology.

§ Department of Molecular Biology.

|| Present address: NuVas, LLC, 11545 Sorrento Valley Rd., Suite 305B, San Diego, CA 92121.

[1] Abbreviations: TF, tissue factor; VII/VIIa, coagulation factor VII/VIIa; FFR-VIIa, VIIa modified with the active site inhibitor Phe-Phe-Arg chloromethyl ketone; X/Xa, coagulation factor X/Xa; PC, phosphatidylcholine vesicles; PCPS, phosphatidylcholine/phosphatidylserine vesicles.

10.1021/bi982254r CCC: $18.00
Published on Web 01/27/1999

Gly (*9*) replacement are poorly activated by TF·VIIa. The hereditary Gla-14 → Lys mutation has further been shown to display a selective loss of activation by TF·VIIa, with little impairment of phospholipid binding or of the ability to be activated by the intrinsic X activation complex (*10*). Second, site-directed, amino-terminal deletion of the X Gla-domain severely impairs the activation by the soluble TF_{1-218}·VIIa complex, implying that the X Gla-domain may be involved in protein−protein, rather than in phospholipid, interactions during the docking with TF·VIIa (*11*). Third, TF residues Lys-165 and Lys-166 contribute to protein−protein interactions (*12*, *13*) with the macromolecular substrate X Gla-domain (*14*).

The Gla-domain of VIIa is also essential for function of the TF·VIIa complex. Deletion of the Gla-domain of VIIa reduces the extent of binding to cell surface TF, thereby virtually abolishing cell surface activation of macromolecular substrate X (*15*). Although deletion of the Gla-domain decreases the affinity for TF, it does not affect the TF-induced enhancement of VIIa's amidolytic function upon formation of the TF·desGlaVIIa complex, indicating that the VIIa protease domain properly docks with the cofactor TF (*16*). However, the TF·desGlaVIIa complex is defective in macromolecular substrate interaction whether in the presence or absence of phospholipid, inferring that the VIIa Gla-domain contributes to protein−protein interactions with substrate (*16*). Gla-domain-deleted VIIa has nearly normal proteolytic function in the absence of cofactor TF (*17*), and mutations in the interface of TF with the VIIa Gla-domain influence docking of the various macromolecular substrates (*13*). Taken together, these data lead to the hypothesis that the functional role of VIIa's Gla-domain in facilitating macromolecular substrate activation requires proper orientation and presentation by the cofactor TF.

To characterize the precise role of the VIIa Gla-domain in macromolecular substrate docking, we have generated and characterized a set of site-directed mutants of the VIIa Gla-domain. This analysis provides experimental evidence that shows that specific residues of the VIIa Gla-domain play a critical role in X activation that is dependent on a properly folded Gla-domain of the macromolecular substrate. To provide insight into the molecular details for recognition of the substrate Gla-domain, we have generated computational models for docking of the X Gla-domain with TF·VIIa. The high-ranking solutions suggest interactions of the X Gla-domain with both TF and the cofactor-bound VIIa Gla-domain. These data provide novel insight into the molecular details of the multiple interactions of the macromolecular substrate Gla-domain with the TF·VIIa complex and advance the general understanding of how cofactor proteins mediate their effects on protease function.

MATERIALS AND METHODS

Proteins. Full-length recombinant human TF_{1-263} was produced from insect cells and reconstituted into 30% phosphatidylserine/70% phosphatidylcholine (TF/PCPS) or 100% phosphatidylcholine (TF/PC) vesicles, as described previously (*18*). Molar concentrations of phospholipid-reconstituted TF are based on the amount of TF available on the outside of the vesicles, based on titrations with wild-type VIIa to maximal amidolytic activity. The soluble extracellular domain of TF, TF_{1-218}, was expressed in *Escherichia coli* and purified and refolded from inclusion bodies, as described previously (*19*). The protein concentration was determined by bicinchoninic acid assay (Pierce Chemical Co., Rockford, IL), and molar concentrations were based on the calculated molecular mass of 25 000 Da. X was purified from plasma, followed by immunoaffinity chromatography on immobilized monoclonal antibody F21-4.2 to reduce contamination by VII, as described previously (*5*). Recombinant wild-type and mutant VII were expressed in Chinese hamster ovary (CHO) cells and purified by sequential monoclonal antibody and ion exchange chromatography, as described previously (*18*). Protein concentrations for VII and X were determined by bicinchoninic acid assay (Pierce Chemical Co.) and converted to molar concentrations on the basis of the calculated molecular mass.

Expression and Purification of Recombinant X. A full-length cDNA clone for X was kindly provided by W. Church (*20*). The coding sequence was subcloned into pED4 (*21*) and mutated at the propeptide position Thr-2 to Arg to facilitate cellular processing (*22*). To eliminate heterogeneity from glycosylation of the activation peptide, both glycosylation attachment sites were eliminated by mutagenesis of Asn-181 and Asn-191 (residue numbering based on ref *20*) to Ala and Asp, respectively. DHFR-deficient Chinese hamster ovary cells were stably transfected with the X cDNA together with a construct encoding a soluble form of the processing enzyme furin/PACE (*23*) to enhance proper processing into the mature two-chain zymogen form of X. Recombinant proteins were produced in serum-free cultures in spinner flasks, employing Excel 301 (JRH Scientific) supplemented with 200 ng/mL vitamin K_3 and 10 units/mL Trasylol. Conditioned culture medium was adjusted to 1 mM benzamidine prior to passing over immobilized anti-X monoclonal antibody F21-4.2C for isolation of the recombinant protein. After adsorption, the antibody column was washed with 1 M NaCl, 10 mM EDTA, and 1 mM benzamidine (pH 8), followed by elution of the bound X with 2 M guanidine hydrochloride and 1 mM benzamidine. The protein solution was immediately dialyzed against 20 mM Tris and 150 mM NaCl (pH 7.4) (TBS) containing 1 mM benzamidine. We observed heterogeneity of the light chain of the recombinant protein under reducing conditions. This heterogeneity was attributed to differing degrees of γ-carboxylation or degradation. To separate these species of recombinant X, the fraction with affinity for barium citrate precipitate was isolated, as follows. The dialyzed protein was adjusted to a concentration of 0.6 mg/mL in the same buffer, followed by addition of sodium citrate to 16 mM. On ice, a 1 M $BaCl_2$ solution was added dropwise to a final concentration of 100 mM while the mixture was stirred vigorously. The precipitate was harvested by centrifugation at 5000*g* for 1 h and resuspended at approximately 1−2 mg/mL in 0.1 M Tris, 0.2 M sodium citrate, and 1 mM benzamidine (pH 8.0) by rotating overnight. After residual precipitate was eliminated by centrifugation, the eluate was dialyzed extensively against TBS and stored at −70 °C. A final pass over a benzamidine Sepharose column equilibrated with TBS was used to eliminate trace contaminants of Xa that may have been generated during production or purification of the recombinant protein. The barium citrate precipitate supernatant was treated accordingly and stored in TBS at −70

°C. Amino-terminal sequencing of the recombinantly produced X demonstrated the expected sequence ANSFLEEMKK for the barium citrate-precipitated material. The average yield for the two Glu residues was <4% of the average yield for the subsequent Lys residues. Since γ-carboxylation reduces the yield of Glu residues, these data demonstrate that >96% of Glu-6 and -7 were γ-carboxylated. The light chain sequence of recombinant X in the barium citrate supernatant had one predominant sequence, i.e., KGHLEREXME, which corresponds to a truncated light chain starting at X Gla-domain residue Lys-10. Minor sequences indicated that Lys-10 was additionally removed in certain molecules of the preparation. The cleavage of the Lys-9−Lys-10 bond likely occurred via cellular processing proteases under production cell culture conditions. This truncation must severely impair Gla-domain folding, since the core Ca^{2+}-coordinating Gla residues at positions 6 and 7 and the hydrophobic membrane binding residues Phe-4, Leu-5, and Met-8 are removed. We refer to this fraction as truncated recombinant X, as compared to the barium citrate precipitatable full-length recombinant X.

Functional Assays. Activation of X by TF·VIIa was analyzed in a linked functional assay at 37 °C. After a typical 5 min preincubation of the indicated concentrations of TF and VIIa to allow for complex formation, X was added to initiate the reaction which was quenched with 100 mM EDTA. Xa formation in samples was assessed with the chromogenic substrate Spectrozyme FXa. Typically, a fixed concentration of enzyme or cofactor was saturated with increasing concentrations of the respective ligand, and X was added at the indicated fixed concentration. For the determination of the kinetic parameters K_M and k_{cat} for X hydrolysis by TF·VIIa, a fixed concentration of TF/PCPS or TF/PC (200 pM) was combined with excess wild-type or mutant VIIa (1 nM) in Hepes-buffered saline [10 mM Hepes and 150 mM NaCl (pH 7.4)], 5 mM $CaCl_2$, and 0.2% bovine serum albumin. The substrate X concentration was varied from 0.2 nM to 10 μM. Initial rate data were fitted to the Michaelis−Menten equation. Amidolytic function of wild-type or mutant VIIa (5 nM) was measured in the presence of increasing concentrations of soluble TF_{1-218} (0.5−100 nM) with 0.5 mM chromogenic substrate Chromozyme tPA (Boehringer Mannheim) in Tris-buffered saline, 5 mM $CaCl_2$, and 0.2% bovine serum albumin (pH 8.0) at ambient temperature.

Mutants were generated by site-directed mutagenesis; the sequence was confirmed by DNA sequencing, and the mutational effect was characterized in transient transfection experiments in which a linked functional assay was employed, as described in detail previously (*5*, *24*). Briefly, TF or VII was transiently expressed in Chinese hamster ovary cells. For the analysis of TF mutants, cells were harvested after 48 h, and for the analysis of VII mutants, serum-free culture supernatant was collected for 48 h. The concentrations of TF and VII were determined by immunoassay of cell lysates or supernatants, respectively. To characterize TF mutants, octyl glycoside lysates of cells were prepared and analyzed in the functional assay with recombinant VIIa. Recombinant TF reconstituted in PCPS in combination with wild-type or mutant VII in serum-free supernatant was used in the functional assay to characterize the VII mutants. A fixed concentration of TF (5 pM) was incubated with increasing concentrations of VII, and activation of X (100 nM) was assessed with an end-point method. The rate data were fitted to the single-site binding equation (*5*) to yield apparent K_D and maximal rates of Xa formation at saturation, as measures for cofactor−enzyme affinity and proteolytic activity, respectively.

Surface Plasmon Resonance Analysis. The kinetics of binding were analyzed with BIAcore 2000 instruments at ambient temperature. A noninhibitory monoclonal antibody to TF (TF9-10H10) was directly immobilized by coupling through free amino groups to a carboxylated dextran matrix, activated with a mixture of *N*-hydroxysuccinimide (NHS) and *N*-ethyl-*N*′-[3-(diethylamino)propyl]carbodiimide (EDC). Kinetics of binding of wild-type and mutant VIIa to TF were determined by capturing full-length TF to the antibody, as previously described (*25*). Experiments were performed in HBS, 5 mM $CaCl_2$, 0.005% surfactant P20, and 3 mM CHAPS at a flow rate of 30 μL/min. For measuring binding to soluble TF_{1-218}, CHAPS was omitted from the buffers. Association rate constants (k_s) were calculated from five or more concentrations of VIIa. The k_{on} was determined from the concentration dependence of k_s and the k_{off} from analysis of the response curve upon return to buffer flow.

SurfDock Computational Docking of the X Gla-Domain with TF·VIIa. SurfDock, an automated protein−protein docking program described in full elsewhere (*26*), predicts the relative positions of two interacting protein molecules with known three-dimensional structures. We used this approach successfully to predict the structural complex of β-lactamase (BLIP) with its inhibitory protein (RTEM) (*27*), prior to the experimental structure determination. In this docking approach, atomic interactions are abstracted onto the molecular surfaces of the interacting proteins. These surfaces and surface properties, e.g., hydrophobicity and electrostatic potential, are represented as expansions of spherical harmonic functions. The resolution of the surface representation is controlled by varying the number of terms used in the expansion. When possible protein−protein complexes are being sought, low-resolution representations are evaluated first, and progressively higher-resolution models are used sequentially. An evolutionary programming (EP) technique is used for exploring the configurational search. In EP, we use a population of candidate solutions which undergo mutation, competition, and selection to find the global optimum of a given function. Each member of the population encodes the independent variables of the function to be optimized and is also known as a state vector. In this approach, the function to be optimized consists of shape complementarity, hydrophobicity, electrostatic potential, and van der Waals overlap. In this docking approach, one molecule is considered to be fixed and the other molecule is mobile and positioned relative to it. The independent variables of the pseudo-energy function describe the geometric transformation that is applied to the mobile protein to form the complex. Each member of the population encodes a different position of the mobile structure. Each member of the population is scored using the pseudo-energy function to determine the quality of the complex. In probabilistic selection, we choose members of the population to be used in future generations, and new members of the population are generated by modifying the position and orientation state variables using normally distributed perturbations.

SurfDock was used to predict the docking of the X Gla-domain with the TF·VIIa complex. The coordinates of the TF·VIIa complex (*6*) were taken from the Brookhaven Protein Data Bank (1dan). A homology model of the X Gla-domain from residues 1−48 was based on the structure of the VIIa Gla-domain in the TF·VIIa structure. The Gla-domain of X was modeled using the Homology module of the MSI software package on Silicon Graphics workstations. The homology model of the Gla-domain of X was energy optimized using a conjugate gradient minimizer to remove any side chain clashes. For computational docking of the X Gla-domain with TF·VIIa, a solvent-excluded surface surrounding the C-module of TF and the bound Gla-domain of VIIa (residues 18−48) was created with the MSMS program (*28*). For this surface, a set of spherical harmonic surfaces of various resolutions were generated. We also generated a similar set of spherical harmonic surfaces for the Gla-domain of Xa, based upon its solvent-excluded surface. To these spherical harmonic surfaces we mapped electrostatic potentials, which were calculated on the basis of a distance-dependent dielectric with no distance cutoff, and residue-based hydrophobicities developed by Nozaki and Tanford (*29*) and Kyte and Doolittle (*30*). In our docking computation, we considered TF·VIIa-Gla-domain complex the fixed molecule and the surface of the Xa Gla-domain the mobile molecule. At the end of 200 generations of SurfDock calculation, we visually analyzed the top 50 scoring complexes. Some complexes showed an orientation of the hydrophobic tip of the Gla-domain distant from and oriented away from the phospholipid membrane surface. These solutions were considered unlikely for the following reasons. First, this orientation of the Gla-domain would be disfavorable for interactions of the X scissile bond with the catalytic cleft of VIIa. Second, this mode of docking would be inconsistent with the experimental evidence demonstrating that phospholipid binding of the X Gla-domain enhances the activation by TF·VIIa. These docking solutions were therefore excluded. The top five eliminated docking solutions had scores of −751, −716, −704, −609, and −568. The remaining top 10 scoring complexes were subjected to detailed structural analysis, and the top four solutions are discussed in detail in this paper.

RESULTS

Normal TF Binding of VIIa$_{Ala-32Ala-36}$. On the basis of the hypothesis that basic residues in the VIIa Gla-domain cooperate with the adjacent, electropositive TF carboxyl-terminal module in providing a docking site for the X Gla-domain, we generated a VIIa mutant that incorporated Ala replacements for both Lys-32 and Arg-36. Since a charge reversal mutation of Lys-32 has recently been shown to enhance, rather than to inhibit, VIIa's coagulant function (*31*), we attribute functional deficits of the double mutant to the effects of the Arg-36 replacement by Ala. By surface plasmon resonance analysis using antibody-captured full-length TF or soluble TF_{1-218}, we characterized the TF binding of mutant and wild-type zymogen forms, active enzymes, and catalytic site-modified VIIa (Table 1). The binding kinetics for mutant VII/VIIa were similar to those of the wild-type VII/VIIa analyzed in parallel. Normal binding is further demonstrated by the TF-dependent enhancement of amidolytic function that occurred with similar dose dependence for wild-type and mutant VIIa (Figure 1). These data also show that the TF-induced allosteric changes in the VIIa protease domain, which enhance VIIa's amidolytic function, are not significantly influenced by the mutations in the Gla-domain of VIIa.

Table 1: Binding Kinetics for TF Interaction of VIIa$_{Ala-32Ala-36}$[a]

	k_{on} (x10^5 M^{-1} s^{-1})	k_{off} (x10^4 s^{-1})
Binding to TF_{1-263}		
VII		
wild-type	2.7 ± 0.2	8.2 ± 0.5
mutant	1.7 ± 0.1	9.6 ± 1.1
VIIa		
wild-type	1.7 ± 0.3	11 ± 0.7
mutant	2.1 ± 0.1	7.0 ± 1.8
FFR-VIIa		
wild-type	2.3 ± 0.2	3.1 ± 0.3
mutant	2.2 ± 0.5	3.8 ± 0.3
Binding to TF_{1-218}		
VII		
wild-type	2.0 ± 0.2	50 ± 12
mutant	0.8 ± 0.1	34 ± 2.8
VIIa		
wild-type	1.4 ± 0.8	16 ± 2.2
mutant	1.1 ± 0.1	16 ± 1.0
FFR-VIIa		
wild-type	2.0 ± 0.3	4.6 ± 0.6
mutant	1.1 ± 0.1	5.5 ± 0.7

[a] Mean ± standard deviation ($n = 3$).

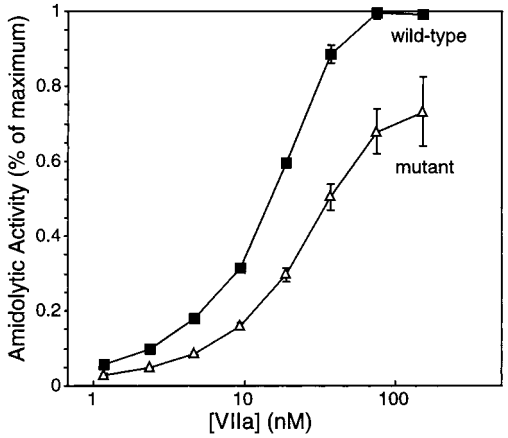

FIGURE 1: Amidolytic activity of VIIa$_{Ala-32Ala-36}$. Amidolytic function was analyzed at a fixed concentration of soluble TF_{1-218} (5 nM) and the indicated concentrations of wild-type or mutant VIIa with the chromogenic *p*-nitroanilide substrate Chromozyme tPA (0.5 mM). Mean ± standard deviation ($n = 3$).

Mutation of the VIIa Gla-Domain Reduced Proteolytic Function Independent of Phospholipid Interactions. Activation of macromolecular substrate X was analyzed in the presence or absence of different phospholipid surfaces (Figure 2). The extent of activation of plasma-derived X by the complex of TF with the VIIa mutant was severely reduced on both negatively charged and neutral phospholipids (Figure 2A). Interactions of the substrate or enzyme Gla-domain with the negatively charged phosphatidylserine headgroups are thus not perturbed by the mutation in the VIIa Gla-domain. Kinetic analysis showed a 3-fold decreased affinity for substrate X, as measured by the K_M, and a 6−10-fold reduced k_{cat} (Table 2). Activation of X was reduced to at least the same relative extent in the absence of phospholipid, as demonstrated by the analysis with detergent-solubilized full-length TF or with soluble TF_{1-218} (Figure

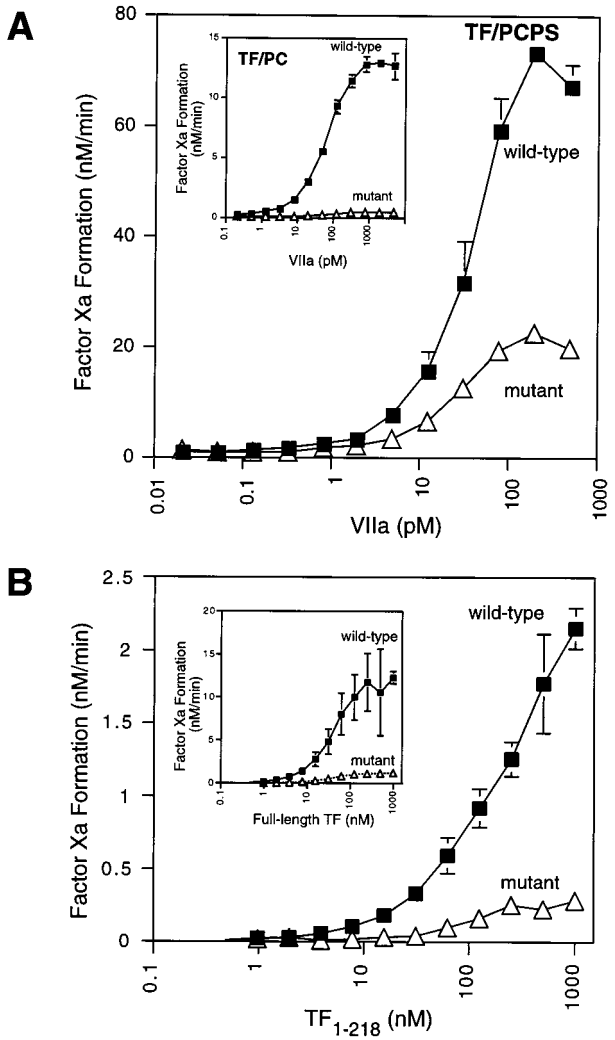

FIGURE 2: Analysis of activation of plasma-derived X by wild-type and mutant VIIa under various membrane and cofactor conditions. (A) Activation of 1 μM X by the indicated concentration of wild-type VIIa or $VIIa_{Ala-32Ala-36}$ and 200 pM TF reconstituted into PCPS vesicles or (inset) activation of 5 μM X in the presence of 200 pM TF in pure PC vesicles. (B) Activation of 1 μM X by 100 nM wild-type VIIa or $VIIa_{Ala-32Ala-36}$ in the presence of increasing concentrations of soluble TF_{1-218} or (inset) detergent-solubilized full-length TF. Mean $\pm$ standard deviation ($n = 3$).

Table 2: Kinetic Parameters for X Activation by $VIIa_{Ala-32Ala-36}$[a]

	K_M	k_{cat}
TF/PC[b]		
wild-type VIIa	11.1 $\pm$ 2.8 μM	1.55 $\pm$ 0.15 s^{-1}
$VIIa_{Ala-32Ala-36}$	28.1 $\pm$ 5.4 μM	0.15 $\pm$ 0.05 s^{-1}
TF/PCPS		
wild-type VIIa	69 $\pm$ 25 nM	7.40 $\pm$ 0.45 s^{-1}
$VIIa_{Ala-32Ala-36}$	152 $\pm$ 55 nM	1.20 $\pm$ 0.30 s^{-1}

[a] Mean $\pm$ standard deviation ($n = 3$). [b] Two hundred picomolar TF reconstituted into phosphatidylcholine (PC) or phosphatidylcholine/phosphatidylserine (PCPS) with 1 nM VIIa.

2B). The specific role of VIIa Gla-domain residue Arg-36 in supporting macromolecular substrate activation is thus not dependent on phospholipid interactions with the VIIa Gla-domain. Rather, these data indicate that specific residues of the VIIa Gla-domain participate in protein−protein interactions of the TF·VIIa complex with macromolecular substrate, consistent with the effect observed upon deletion of the VIIa Gla-domain (*16*). The extent of activation of X by the VIIa Gla-mutant in the absence of TF was only slightly reduced relative to that of wild-type VIIa. Mutant VIIa (250 nM) activated X (2 μM) with a rate of 0.24 $\pm$ 0.03 nmol/min in the absence and of 4.6 $\pm$ 1.1 nmol/min in the presence of 50 μM mixed phospholipid, as compared with rates for wild-type VIIa of 0.30 $\pm$ 0.01 and 10.3 $\pm$ 3.9 nmol/min ($n \geq 3$), respectively. These data are consistent with the analysis of Gla-domain-deleted VIIa that displayed a <2-fold reduced rate of X activation in comparison to wild-type VIIa, when analyzed in the absence of cofactor (*17*). The functional importance of the enzyme VIIa Gla-domain in activation of macromolecular substrate is thus cofactor-dependent.

VIIa Gla Residue Arg-36 Interactions Require a Functional Gla-Domain of Macromolecular Substrate. Since TF residues Lys-165 and Lys-166 located in close proximity to Arg-36 have been suggested to interact with the X Gla-domain (*14*), we investigated whether the VIIa Gla-domain mutant is defective in activating macromolecular substrate that lacks a properly folded Gla-domain. In our preparation of recombinant X, we separate X that is truncated by limited proteolysis in the Gla-domain from full-length X that has normal divalent metal ion binding properties. As observed with plasma-derived X, full-length recombinant X was activated with significantly reduced rates by the mutant VIIa in complex with phospholipid-reconstituted TF, as compared to the activation rates by wild-type VIIa under the same conditions (Figure 3A). Activation of truncated recombinant X by the same concentration of TF·VIIa complex was reduced >100-fold (Figure 3B), consistent with previous studies that showed the importance of the X Gla-domain for efficient activation by TF·VIIa (*11*). Activation of truncated X by the VIIa mutant was compared with that with wild-type VIIa in the presence (Figure 3B) or absence of phospholipid (Figure 3C). Unlike the results with the full-length recombinant X (Figure 3A), no difference was observed between wild-type and mutant VIIa in the activation of the recombinant X with a misfolded Gla-domain due to amino-terminal truncation. These data demonstrate that the functional role of VIIa Gla-domain residue Arg-36 requires a properly folded Gla-domain of the macromolecular substrate X.

SurfDock Solutions for the Interaction of the X Gla-Domain with TF·VIIa. In lieu of a crystallographic solution to the structure of the ternary TF·VIIa·X complex, we addressed the molecular details of the interaction of the X Gla-domain with the TF·VIIa complex by computational docking simulation using the SurfDock suite of programs. A homology model of the X Gla-domain from residues 1−48 was generated on the basis of the structure of the Gla-domain of VIIa (*6*). This model was computationally docked to the complex of the TF carboxyl-terminal module and the VIIa Gla-domain. None of the solutions for docking of the X Gla-domain collided significantly with other structural elements of the complete TF·VIIa complex that included the EGF and protease domains of VIIa. The initial docking solutions were filtered on the basis of the experimental evidence that showed that phospholipid binding of macromolecular substrate greatly enhances assembly with TF·VIIa (*32*), inferring that the exposed hydrophobic residues Phe-4, Leu-5, and Met-8 of the X Gla-domain should be oriented toward the membrane surface. This orientation of the Gla-domain would favor an upright position of the X molecule required for

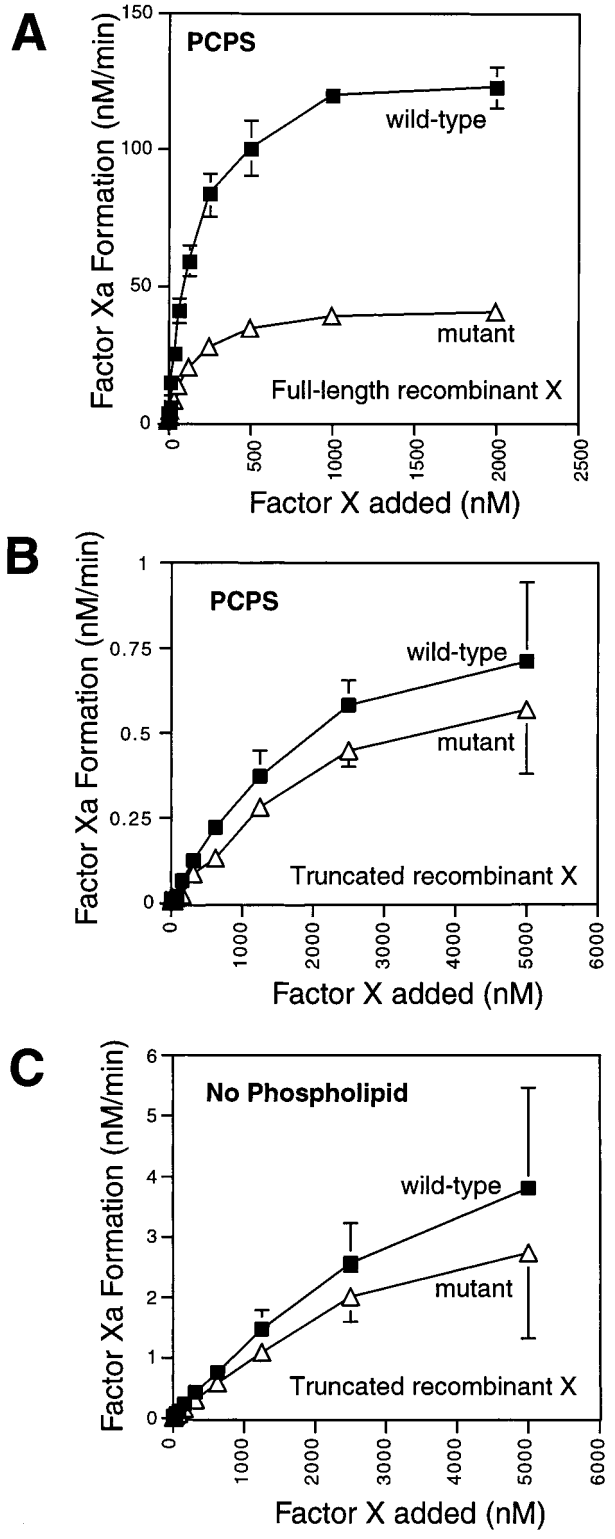

FIGURE 3: (A) Activation of recombinant, full-length X by mutant or wild-type VIIa (1 nM) in complex with phospholipid-reconstituted TF (200 pM). (B) Activation of truncated recombinant X, which has a misfolded Gla-domain, by mutant or wild-type VIIa. Activation of the indicated concentration of truncated X by 1 nM VIIa in the presence of 200 pM TF in PCPS or (C) 50 nM VIIa with 250 nM detergent-solubilized full-length TF. Comparable results were obtained with TF in PC or soluble TF_{1-218}. Mean ± standard deviation ($n = 3$).

presentation of the scissile bond to the catalytic cleft of VIIa (*6*, *33*). Only solutions that were consistent with membrane interactions of the X Gla-domain were considered for the detailed structural analysis.

The four highest-scoring solutions are illustrated in Figure 4, and details of the solutions are summarized in Table 3. The highest-scoring solution also had the largest buried surface area, whereas the second highest-scoring solution had the smallest buried surface area of the four. In part, the high score for the second solution may be due to larger contributions from interactions of hydrophobic side chains, such as the X Gla-domain residues Met-18 and Tyr-44, which contrasts with the other three solutions that are predominantly supported by interactions of side chains that are based on charge complementarity (Table 3). In solutions 1, 3, and 4, Gla-14 of X was consistently found to dock with a common collision surface generated by TF and the VIIa Gla-domain. X Gla-14 is close to either VIIa Gla-domain residue Lys-38 or the immediately adjacent TF residue Ser-163. In solution 2, Gla-14 makes a more peripheral contact with Lys-169 which is distant from the VIIa Gla-domain (Figure 4). The dissimilarity of solutions 1, 3, and 4 versus solution 2 is also illustrated by other X Gla-domain residues. X Glu-39 in the former consistently makes contacts with TF Tyr-156, whereas the contact residue for TF Tyr-156 in solution 2 is X Gla residue Tyr-44 of the aromatic stack helix. X Asp-35 contacts TF Thr-167 in solutions 1 and 3, whereas TF Thr-167 contacts Met-18 in solution 2.

In solution 2, the X Gla-domain does not contact the VIIa Gla-domain. The high-affinity Ca^{2+}-binding site of the X EGF-1 domain immediately follows the aromatic stack helix, which is part of the docked X Gla-domain model. The EGF-1 Ca^{2+} site could potentially make contacts with VIIa Gla-domain residue Lys-38 or Arg-36 in the orientation of the docked X Gla-domain in solution 2. More extended interactions of the X Gla-domain with the VIIa Gla-domain are only predicted for the other three solutions. In these, the X Gla-domain occupies overall a very similar surface region of TF and the VIIa Gla-domain. The X Gla-domain orientation in each of these solutions, nevertheless, is quite different, orienting the hydrophobic tip of the X Gla-domain at variable distances from the VIIa Gla-domain (Figure 4). It is possible that each of these different docking modes of the X Gla-domain is compatible with the assembly of membrane-bound macromolecular substrate with the same surface region of TF·VIIa, but that one of the solutions is the preferred docking position for macromolecular substrate cleavage.

All solutions indicate contacts with TF residues that have been implicated in macromolecular substrate activation, i.e., Ser-163, Lys-165, and Lys-166 (*12*, *34*). Solution 2 indicates only close contacts with TF, whereas interactions with specific residues of the VIIa Gla-domain are consistently shown by solutions 1, 3, and 4. VIIa Glu-35 makes contacts with X Lys-10, Lys-36, or Lys-43 and Met-18 in solution 1, 3, or 4, respectively. The normal clotting function of mutants at this position (*35*) supports the possibility that this contact may have little functional importance for macromolecular substrate activation, as also shown below. The VIIa Gla-domain residue Lys-38 contacts X Gla-14 in solutions 1 and 3, whereas the X Gla-14 side chain in solution 4 is in a similar, but more buried, position that leads to contacts with TF Ser-163 and also VIIa Arg-36. Very subtle allosteric changes in the orientation of the VIIa Gla-domain as a consequence of induced fit conformational changes that follow initial binding of the X Gla-domain may favor

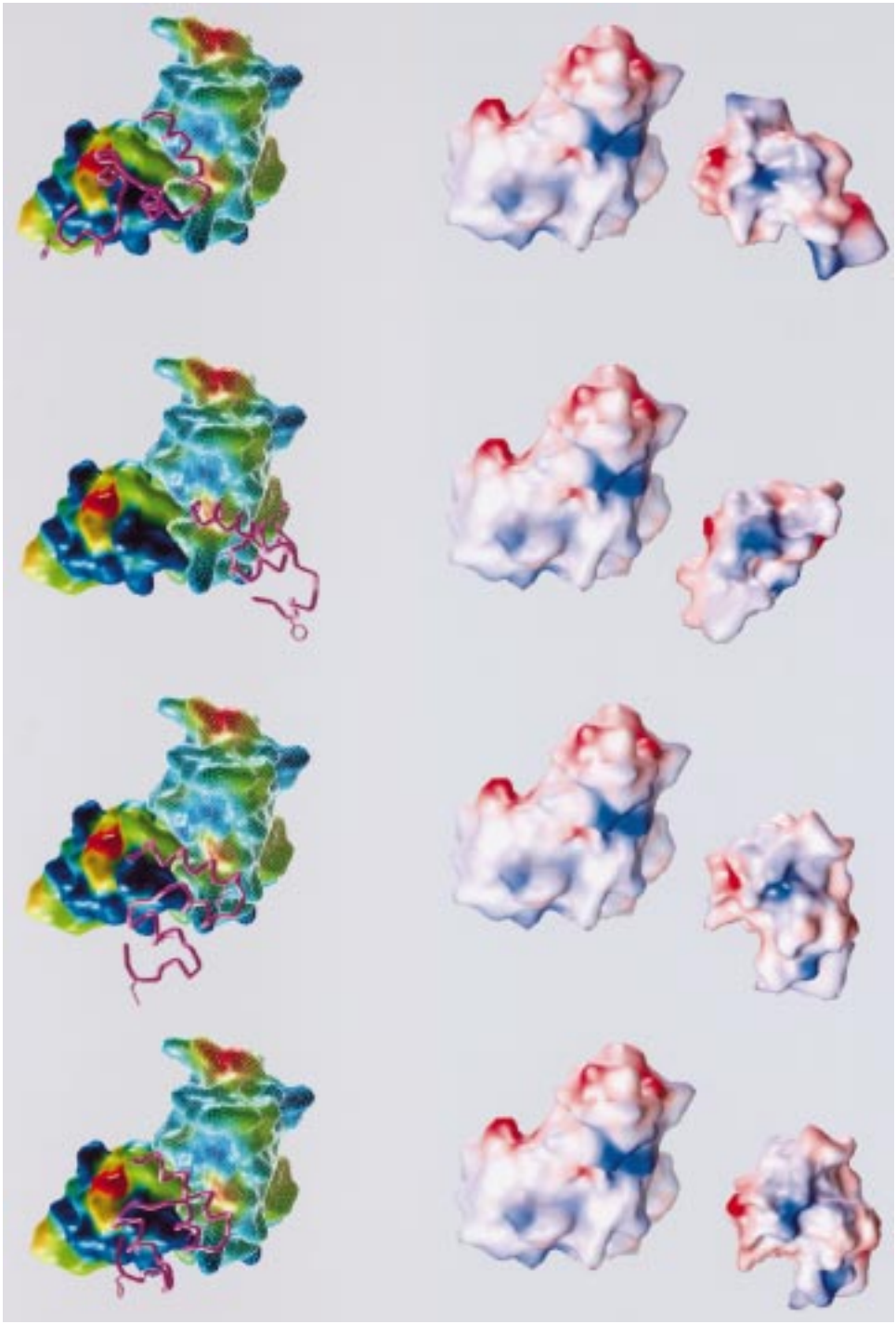

FIGURE 4: Views of the four highest-ranking (from top to bottom) computational solutions for the docking of the X Gla-domain with TF·VIIa. In the left panel, the X Gla-domain is displayed as a backbone tube with the side chains of Phe-4, Gla-14, and Lys-36. The surface of the TF carboxyl-terminal module is displayed as a grid, and the surface of the VIIa Gla-domain is displayed solid with colors encoding increasing hydrophobicity (yellow to red) or increasing hydrophilicity (green to blue). Spherical harmonic surfaces, as used in SurfDock, are shown. The right panel shows an open book display of the charge properties of the interfaces of TF·VIIa with the X Gla-domain for each of the docking position. The X Gla-domain is flipped to the right by 180° along a vertical axis that runs at the right edge of the TF·VIIa complex, shown in a fixed position and the same orientation as in the left panel. The calculated electrostatic potential is displayed from electronegative (red) to electropositive (blue). In solutions 3 and 4, Gla-14 of the X Gla-domain is visible as a weak electronegative protruding area between the two strongly basic clusters.

interaction of X Gla-14 with either VIIa Arg-36 or VIIa Lys-38, which are in close spatial proximity to one another. Docking solutions 1 and 3 thus do not exclude interactions of X Gla-14 with VIIa Arg-36 that, based on the above-described functional analysis, make important contributions to X Gla interactions.

Evidence for a Critical Role of Charge Complementarity in the Docking of the X Gla-Domain with TF·VIIa. Individual site specific mutations in the VIIa Gla-domain were generated to further define the importance of individual charged residue side chains for X macromolecular substrate activation. Ala substitutions for VIIa Lys-18, Arg-28, Lys-32, Asp-

Table 3: Summary of the Computational Docking Solutions for X Gla-Domain Interactions with TF·VIIa

	solution 1	solution 2	solution 3	solution 4
composite score	−843	−735	−611	−603
buried surface area (Å^2)	588	390	559	516
side chains within 3-5 Å of the Gla-*X* residue				
Gla-14	VIIa Lys-38	TF Lys-169	VIIa Lys-38	TF Ser-163, VIIa Arg-36
Glu-39	TF Tyr-156, TF Lys-201		TF Tyr-156, TF Lys-165	TF Tyr-156, TF Thr-167
Lys-43	TF Asp-204, TF Gln-110		TF Asp-204, VIIa Glu-35	VIIa Glu-35
Met-18		TF Thr-154, TF Thr-167		VIIa Glu-35
Asp-35	TF Thr-167		TF Thr-167	
Lys-36	TF Asp-204		VIIa Glu-35	
Asn-38			TF Lys-201	TF Lys-201
Asn-42			TF Gln-110	TF Gln-110
Asp-46			TF Gln-110	TF Thr-203
Lys-10	VIIa Glu-35			
Gla-19		TF Lys-166		
Gla-20		TF Tyr-157		
Gla-32	TF Ser-163			
Asp-33	TF Lys-165			
Tyr-44		TF Tyr-156		
Asp-48		TF Lys-165		

Table 4: Functional Characterization of Site-Directed Mutants of TF and VIIa

mutated residue	maximum rate of X activation[a] (pmol of Xa formed/s)	K_{Dapp} for TF·VIIa binding (pM)
wild-type VIIa control	10.4 ± 0.7	5 ± 1
VIIa Lys-18 → Ala	10.5 ± 0.5	7 ± 3
VIIa Arg-28 → Ala	8.2 ± 0.1	9 ± 1
VIIa Lys-32 → Ala	7.2 ± 0.1	6 ± 1
VIIa Asp-33 → Ala	7.5 ± 0.4	9 ± 1
VIIa Glu-35 → Ala	10.0 ± 2.0	8 ± 2
VIIa Arg-36 → Ala	1.9 ± 0.3	6 ± 2
VIIa Lys-38 → Ala	9.9 ± 0.6	6 ± 1
wild-type TF control	3.9 ± 0.1	6 ± 1
TF Thr-167 → Lys	10.1 ± 0.1	7 ± 2
TF Ala-168 → Lys	4.5 ± 0.8	7 ± 1

[a] Determined at 5 pM TF and varying VIIa concentrations to saturation, with X at 100 nM. Mean ± standard deviation ($n = 3$).

33, Glu-35, and Lys-38 had only minor effects on the rate of X activation, although a <2-fold increased K_D was observed for some of the mutants (Table 4). This may indicate that some of the charged side chains aid in assembly of the TF·VIIa complex, as previously shown for one of these residues, Glu-35 (*35*). The only mutant that showed a severely reduced level of X activation in the transient transfection assay was the VIIa Arg-36 → Ala mutation, consistent with the analysis of the purified mutant protein described above. To further test the charge complementarity of the X Gla-domain interaction with TF·VIIa, we introduced a positively charged Lys side chain for TF Thr-167 which is predicted to be close to either X Asp-35 or X Glu-39 by solutions 1 and 3, or 4, respectively. Mutation of TF Thr-167 to Lys increased the rate of X activation 2-fold (Table 4). Lys replacement of the adjacent residue Ala-168 did not enhance proteolytic function, indicating that charge complementarity of specific contact residues, rather than a general increase in electropositivity of the local surface environment, is responsible for the enhanced function. The gain of function of the Thr-167 mutant lends support to the computational docking solutions, which suggest that multiple interactions of residue side chains with complementary charges are critical for docking of the X Gla-domain with TF·VIIa.

DISCUSSION

In this study, we characterize macromolecular substrate docking with the TF·VIIa complex. We demonstrate that Ala mutation of the VIIa Arg-36 side chain selectively reduces the extent of macromolecular substrate activation, but neither affects TF binding or the amidolytic function of VIIa. The reduced proteolytic function of the VIIa Arg-36 mutant was independent of potential phospholipid interactions of the VIIa Gla-domain, but dependent on the presence of TF. The cofactor TF thus appears to play a critical role in promoting protein−protein interactions of the VIIa Gla-domain with the macromolecular substrate. The VIIa Arg-36 mutant was defective in the proteolytic activation of X only when the substrate's Gla-domain was properly folded. Recombinant X with a truncated Gla-domain was activated by $VIIa_{Ala-32Ala-36}$ at rates indistinguishable from that of wild-type VIIa. Thus, Arg-36 must either be required for proper overall orientation of the VIIa Gla-domain to generate an optimal charge field for docking of the X Gla-domain with TF·VIIa or directly associate with the X Gla-domain.

Ala mutation of Arg-36 produced the most significant reduction of function among the described charged residue side chain mutations in the VIIa Gla-domain that included Lys-18, Arg-28, Lys-32, Asp-33, Glu-35, and Lys-38 (Table 4). The computational docking solutions propose that Glu-35 and Lys-38 may contact the X Gla-domain. Consistent with earlier reports (*35*), we find no significantly reduced proteolytic function for the Glu-35 mutant, and the Lys-38 mutant was also normal in macromolecular substrate X activation. The predicted docking site for the X Gla-domain is a region of the TF·VIIa complex structure that shows some disorder, in particular the TF segment of residues 158−164 and VIIa Glu-35 (*6*). This is consistent with increased local flexibility of the TF·VIIa Gla-domain collision structure which may allow for subtle conformational changes. A slight change in the VIIa Gla-domain orientation could position the Arg-36 side chain, rather than Lys-38, more favorably for interaction with electronegative residue side chains in the X Gla-domain. Experimental evidence from TF mutants in the interface with the VIIa Gla-domain (*13*) or EGF-1 (*36*), and from mutations of the EGF-1 high-affinity Ca^{2+}-

binding site in VIIa (*37*), also indicates that flexibility in docking of the VIIa Gla-domain with TF may influence macromolecular substrate activation. We suggest either that the molecular details provided by the static view of the TF·VIIa complex structure do not represent accurately the recognition structure with which the X Gla-domain assembles or that an initial encounter of the X Gla-domain with the TF C-module induces subtle reorientations of the VIIa Gla-domain.

Computational docking of the X Gla-domain to TF·VIIa predicts an extended contact of approximately 500 Å^2 which is similar to the size of the VIIa protease domain interface with TF and which even exceeds the buried surface area between the VIIa Gla-domain and TF. The X Gla-domain has good shape and charge complementarity with the predicted docking surface that is formed by the merged surface of the VIIa Gla-domain with the TF carboxyl-terminal module. We find a gain of function upon introduction of a Lys side chain for TF Thr-167, which is in predicted close proximity to negatively charged residues of the docked X Gla-domain, demonstrating that specific charge complementary side chain interactions support macromolecular substrate docking. Charge reversal of the basic TF residues Lys-165 and Lys-166 (*14*) and the introduction of a negatively charged Asp side chain for TF Ser-162 (*34*) also profoundly reduce proteolytic function, likely by charge repulsion of electronegative, surface-exposed side chains of the X Gla-domain that dock with TF·VIIa. The available experimental data are thus consistent with the computational docking solutions that predict important charge complementary interactions of the X Gla-domain with an extended binding site formed by TF and the VIIa Gla-domain.

It is striking that computational docking solution 2 predicts interactions that are quite dissimilar to those of the other three high-ranking solutions. The X Gla-domain residues that make close contacts in solution 2, i.e., Gla-14, Gla-19, Gla-20, Met-18, Tyr-44, and Asp-48, are fully conserved in the alternative macromolecular substrate factor IX, and all but Met-18 are conserved in VII, which is also activated by VIIa in a TF-dependent manner (*38*, *39*). In contrast, several contacts that are predicted in solutions 1, 3, and 4 are not conserved in the alternative substrates, in particular X Glu-39, Lys-43, Asn-38, and Asn-48. It is possible that solution 2 more adequately represents a docking mode of the Gla-domains of the alternative substrates. The light chain of factor IX participates in macromolecular substrate docking with TF·VIIa (*40*), and mutations in the carboxyl-terminal module of TF influence the activation of factor IX and VII (*13*). More importantly, site specific mutations of the VII Gla-domain have recently been shown to lead to accelerated zymogen VII activation by TF·VIIa (*31*). Gla-domain interactions of the alternative substrates thus appear to be of equal importance for macromolecular substrate docking to TF·VIIa, as found with the model substrate X in this study.

In the case of X, solution 2 may represent an alternative docking mode of the X Gla-domain that is relevant for interactions of the product Xa with TF·VIIa. Xa plays an important role in supporting the binding of specific inhibitors, i.e., TFPI-1 (*41*) and the hookworm-derived NAPc2 (*42*), to TF·VIIa. These inhibitors form stable quaternary complexes that include the inhibitor and the ternary TF·VIIa·Xa complex. The kinetics of quaternary complex formation indicate that TFPI-1 preferentially associates with the ternary TF·VIIa·Xa complex (*43*), implying that the ternary complex exists for a sufficient duration. The quaternary complex formation with TFPI-1 is also dependent on TF residues Lys-165 and Lys-166 (*44*) which both are implicated in contacting the X Gla-domain in solution 2. This mode of docking is thus consistent with available data on the binding of Xa in complex with TFPI-1.

Computational docking solutions 1, 3, and 4 suggest interactions of X with the VIIa Gla-domain. We provide biochemical evidence that implicates VIIa Gla-domain residue Arg-36 in the interaction with the X Gla-domain. Since the K_M for X activation increased upon Arg-36 mutation, the function of this VIIa Gla-domain residue must be the support of macromolecular substrate binding. We suggest that the computational solutions may be close allosteric variations for the binding mode of the X Gla-domain during macromolecular substrate docking. It is conceivable that during substrate assembly, one of the binding modes is followed by a second, as a consequence of subtle allosteric effects upon the ligand-induced fit. Note that the computational docking is performed with rigid bodies and thus does not score flexibility aspects. These may be of particular importance for the dynamic situation of substrate assembly and subsequent product release. This study provides conclusive experimental evidence for the importance of interactions between the Gla-domains of the enzyme and substrate during macromolecular substrate docking with TF·VIIa and presents novel insight into potential specific molecular contacts. This knowledge can guide future mutational studies in elucidating the dynamic interactions that regulate substrate assembly and product release, and that allow for the formation of stable quaternary inhibitor complexes of the TF initiation complex.

ACKNOWLEDGMENT

We thank Cindi Biazak, Jennifer Royce, and David Revak for excellent technical assistance, Barbara Parker for preparation of the manuscript, Dr. W. R. Church for the X cDNA, and Dr. A. Rehemtulla for the soluble PACE expression construct.

REFERENCES

1. Davie, E. W., Fujikawa, K., and Kisiel, W. (1991) *Biochemistry 30*, 10363−10370.
2. Betz, A., and Krishnaswamy, S. (1998) *J. Biol. Chem. 273*, 10709−10718.
3. Ruf, W., and Edgington, T. S. (1994) *FASEB J. 8*, 385−390.
4. Martin, D. M. A., Boys, C. W. G., and Ruf, W. (1995) *FASEB J. 9*, 852−859.
5. Dickinson, C. D., Kelly, C. R., and Ruf, W. (1996) *Proc. Natl. Acad. Sci. U.S.A. 93*, 14379−14384.
6. Banner, D. W., D'Arcy, A., Chène, C., Winkler, F. K., Guha, A., Konigsberg, W. H., Nemerson, Y., and Kirchhofer, D. (1996) *Nature 380*, 41−46.
7. Higashi, S., Matsumoto, N., and Iwanaga, S. (1996) *J. Biol. Chem. 271*, 26569−26574.
8. Rudolph, A. E., Mullane, M. P., Porche-Sorbet, R., Tsuda, S., and Miletich, J. P. (1996) *J. Biol. Chem. 271*, 28601−28606.
9. Kim, D. J., Thompson, A. R., and James, H. L. (1995) *Hum. Genet. 95*, 212−214.
10. Watzke, H. H., Lechner, K., Roberts, H. R., Reddy, S. V., Welsch, D. J., Friedman, P., Mahr, G., Jagadeeswaran, P.,

Monroe, D. M., and High, K. A. (1990) *J. Biol. Chem. 265*, 11982−11989.
11. Rezaie, A. R., Neuenschwander, P. F., Morrissey, J. H., and Esmon, C. T. (1993) *J. Biol. Chem. 268*, 8176−8180.
12. Ruf, W., Miles, D. J., Rehemtulla, A., and Edgington, T. S. (1992) *J. Biol. Chem. 267*, 6375−6381.
13. Dittmar, S., Ruf, W., and Edgington, T. S. (1997) *Biochem. J. 321*, 787−793.
14. Huang, Q. L., Neuenschwander, P. F., Rezaie, A. R., and Morrissey, J. H. (1996) *J. Biol. Chem. 271*, 21752−21757.
15. Sakai, T., Lund-Hansen, T., Thim, L., and Kisiel, W. (1990) *J. Biol. Chem. 265*, 1890−1894.
16. Ruf, W., Kalnik, M. W., Lund-Hansen, T., and Edgington, T. S. (1991) *J. Biol. Chem. 266*, 15719−15725.
17. Neuenschwander, P. F., and Morrissey, J. H. (1994) *J. Biol. Chem. 269*, 8007−8013.
18. Ruf, W. (1994) *Biochemistry 33*, 11631−11636.
19. Stone, M. J., Ruf, W., Miles, D. J., Edgington, T. S., and Wright, P. E. (1995) *Biochem. J. 310*, 605−614.
20. Messier, T. L., Pittman, D. D., Long, G. L., Kaufman, R. J., and Church, W. R. (1991) *Gene 99*, 291−294.
21. Kaufman, R. J., Davies, M. V., Wasley, L. C., and Michnick, D. (1991) *Nucleic Acids Res. 19*, 4485−4490.
22. Hamamoto, T., Yamamoto, M., Nordfang, O., Petersen, J. G. L., Foster, D. C., and Kisiel, W. (1993) *J. Biol. Chem. 268*, 8704−8710.
23. Wasley, L. C., Rehemtulla, A., Bristol, J. A., and Kaufman, R. J. (1993) *J. Biol. Chem. 268*, 8458−8465.
24. Schullek, J. R., Ruf, W., and Edgington, T. S. (1994) *J. Biol. Chem. 269*, 19399−19403.
25. Dickinson, C. D., and Ruf, W. (1997) *J. Biol. Chem. 272*, 19875−19879.
26. Duncan, B. S., and Olson, A. J. (1996) in *Evolutionary Programming V: Proceedings of the Fifth Annual Conference on Evolutionary Programming* (Fogel, L. J., and Angeline, P. J., Eds.) MIT Press, Cambridge, MA.
27. Strynadka, N. C., Eisenstein, M., Katchalski-Katzir, E., Shoichet, B. K., Kuntz, I. D., Abagyan, R., Totrov, M., Janin, J., Cherfils, J., Zimmerman, F., Olson, A., Duncan, B., Rao, M., Jackson, R., Sternberg, M., and James, M. N. (1996) *Nat. Struct. Biol. 3*, 233−239.
28. Sanner, M. F., Olson, A. J., and Spehner, J.-C. (1996) *Biopolymers 38*, 305−320.
29. Nozaki, Y., and Tanford, C. (1971) *J. Biol. Chem. 246*, 2211−2217.
30. Kyte, J., and Doolittle, R. F. (1982) *J. Mol. Biol. 157*, 105−132.
31. Shah, A. M., Kisiel, W., Foster, D. C., and Nelsestuen, G. L. (1998) *Proc. Natl. Acad. Sci. U.S.A. 95*, 4229−4234.
32. Ruf, W., Rehemtulla, A., Morrissey, J. H., and Edgington, T. S. (1991) *J. Biol. Chem. 266*, 2158−2166.
33. Edgington, T. S., Dickinson, C. D., and Ruf, W. (1997) *Thromb. Haemostasis 78*, 401−405.
34. Ruf, W., Miles, D. J., Rehemtulla, A., and Edgington, T. S. (1992) *J. Biol. Chem. 267*, 22206−22210.
35. Persson, E., and Nielsen, L. S. (1996) *FEBS Lett. 385*, 241−243.
36. Lee, G. F., and Kelley, R. F. (1998) *J. Biol. Chem. 273*, 4149−4154.
37. Kelly, C. R., Dickinson, C. D., and Ruf, W. (1997) *J. Biol. Chem. 272*, 17467−17472.
38. Neuenschwander, P. F., Fiore, M. M., and Morrissey, J. H. (1993) *J. Biol. Chem. 268*, 21489−21492.
39. Yamamoto, M., Nakagaki, T., and Kisiel, W. (1992) *J. Biol. Chem. 267*, 19089−19094.
40. Zhong, D., Smith, K. J., Birktoft, J. J., and Bajaj, S. P. (1994) *Proc. Natl. Acad. Sci. U.S.A. 91*, 3574−3578.
41. Broze, G. J., Warren, L. A., Novotny, W. F., Higuchi, D. A., Girard, J. J., and Miletich, J. P. (1988) *Blood 71*, 335−343.
42. Stanssens, P., Bergum, P. W., Gansemans, Y., Jespers, L., Laroche, Y., Huang, S., Maki, S., Messens, J., Lauwereys, M., Cappello, M., Hotez, P. J., Lasters, I., and Vlasuk, G. P. (1996) *Proc. Natl. Acad. Sci. U.S.A. 93*, 2149−2154.
43. Baugh, R. J., Broze, G. J., Jr., and Krishnaswamy, S. (1998) *J. Biol. Chem. 273*, 4378−4386.
44. Rao, L. V. M., and Ruf, W. (1995) *Biochemistry 34*, 10867−10871.

BI982254R